

Determination of Activation Energy of Entrance into Micropores: Quenching of the Fluorescence of Pyrene-Doped SiO₂ Sol-Gel Matrices by Oxygen

Joshua Samuel, Yulia Polevaya, Michael Ottolenghi,* and David Avnir*

Institute of Chemistry, The Hebrew University of Jerusalem, Jerusalem 91904, Israel

*Received January 14, 1994. Revised Manuscript Received March 22, 1994**

Pyrene-doped xerogels were prepared by the sol-gel method from tetramethoxysilane (TMOS)/water/methanol mixtures. N₂ and CO₂ adsorption isotherms were determined for the xerogels. The pyrene in acid-catalyzed low TMOS/water ratio xerogels was found to be nonleachable. Yet the excited-state dopant was observed to be completely reactive to O₂ quenching in all samples. This finding is of general importance in relation to applications of sol-gel materials as reactive transparent supports for organic molecules. Penetration rates of oxygen into samples were determined by following the drop in pyrene fluorescence over time, after exposure of a precooled sample to the gas. From this data the activation energy for the penetration of oxygen into a xerogel was assessed and found to be 18 ± 1 kJ/mol. This long-range diffusion value is significantly higher than the activation energy for short-range diffusion of oxygen found previously on mesoporous silica.

Introduction

Doped xerogels formed by the sol-gel method have come under intense research recently.¹ These solid matrices are being studied for a number of uses such as lasing materials,² sensors³ and catalytic supports.⁴ The last two applications rely on the capability of the xerogel to contain the active reagent of interest and allow relatively free passage of a reactant from the surroundings to reach the caged molecule. Basic understanding of the mode of encapsulation in the matrix and the effect of the geometric characteristics of the matrix on the accessibility and the leachability of the dopant is lacking. This study concentrates on a number of xerogels formed from a tetramethoxysilane (TMOS)/water/methanol mixture doped with pyrene, characterized by means of nitrogen and CO₂ adsorption. Reactivity of the caged pyrene toward molecular oxygen was observed by exposing precooled samples of the xerogel to oxygen and observing the quenching of the pyrene fluorescence. The increase in the extent of the quenching of pyrene over time serves as a measure for the rate of diffusion of oxygen into the material. While absolute diffusion rates are impossible to determine by this method, the activation energy for diffusion may be assessed.

Pyrene is a convenient photophysical probe, which has been used extensively in surface science in general⁵ and in sol-gel systems in particular.⁶ For a review of the use of pyrene in these systems see ref 7.

Table 1. Characteristics and Preparation of the Pyrene-Doped SiO₂ Xerogels

xerogel	TMOS/H ₂ O ratio	pH ^a	surface area (m ² /g)	apd (Å)	leached pyrene
A	1/2	4	745 ^b 472 ^c	29	69%
B	1/4	1	435, ^b 590 ^d	>10	none
C	1/2	1	450 ^c	^e	none

^a pH is taken from the calculated concentration of H⁺. ^b N₂ BET surface area. ^c CO₂-BET surface area. ^d N₂ Langmuir surface area. ^e Sample not accessible within measurement time to N₂ at liquid nitrogen temperature.

Experimental Details

Chemicals. Tetramethoxysilane from Fluka was used as received. Methanol (99.9%) and cyclohexane (99+%) were spectroscopic grade from Aldrich and were used as received. Pyrene (99% Aldrich) was further purified by sublimation. Water was millipore filtered triply distilled.

Xerogel Preparation. Samples were prepared from a TMOS/water/methanol mixture in a one-step process. The initial solution compositions and the characteristics of the resultant xerogels are collected in Table 1. The samples were acid catalyzed with HCl and were doped with pyrene using a 1.4 mM solution of pyrene in methanol to a concentration of 2.5–2.9 μmol/g of xerogel. All components were added under stirring, and after several minutes each sample was divided to three separate vials. The vials were covered with aluminum foil and placed in an oven at 50 °C for 4–5 weeks until constant weight of the sample was

* Abstract published in *Advance ACS Abstracts*, August 15, 1994.

(1) For an updated review, see: Avnir, D.; Braun, S.; Lev, O.; Levy, D.; Ottolenghi, M. In Klein, L. C., Ed. *Sol-Gel Optics-Processing and Applications*; Kluwer: Dordrecht, 1994; Chapter 23, p 539.

(2) E.g.: Lebrau, B.; Herlet, N.; Livage, J.; Sanchez, C. *Chem. Phys. Lett.* **1993**, *206*, 15.

(3) E.g.: Eguchi, K.; et al. *Sensors Actuators* **1990**, *B1*, 154. Rottman, C.; et al. *Mater. Lett.* **1992**, *13*, 293.

(4) E.G.: Matsuka, J.; Mizutani, R.; Nasu, H.; Kamiya, K. *J. Ceram. Soc. Jpn.* **1992**, *100*, 599. Rosenfeld, A.; Avnir, D.; Blum, J. *J. Chem. Soc., Chem. Commun.* **1993**, 583.

(5) Lochmuller, C. H.; Wenzel, T. *J. Phys. Chem.* **1990**, *94*, 4230. Krasnansky, R.; Koike, K.; Thomas, J. K. *J. Phys. Chem.* **1990**, *94*, 4521. Wong, A. L.; Hunnicutt, M. L.; Harris, J. M. *J. Phys. Chem.* **1991**, *95*, 4489. Suib, S. L.; Kostapapas, A. *J. Am. Chem. Soc.* **1984**, *106*, 7705. Birenbaum, H.; Avnir, D.; Ottolenghi, M. *J. Phys. Chem.* **1989**, *93*, 2728.

(6) Makishima, A.; Tani, T. *J. Am. Chem. Soc.* **1986**, *69*, 72. Yamanaka, T.; Takahashi, Y.; Kitamura, T.; Uchida, K. *Chem. Phys. Lett.* **1990**, *172*, 29. Matsui, K.; Nakazawa, T. *Bull. Chem. Soc. Jpn.* **1990**, *63*, 11. Kaufman, V. R.; Avnir, D. *Langmuir* **1986**, *2*, 717.

(7) Anpo, M. *Heterogen. Chem. Rev.*, in press. (8) Gregg, S. J.; Sing, K. S. W. *Adsorption Surface Area and Porosity*; Academic Press: New York, 1982.

(9) Sobolik, J. L.; Ludlow, D. K.; Hesserick, W. L. *Fuel* **1991**, *71*, 1195. Jaroniec, M.; Madey, R. *Physical Adsorption on Heterogeneous Solids*; Elsevier: Amsterdam, 1988.

achieved. Note that work with alkoxysilanes should be carried out in a fume hood.

Leaching. Leaching of the pyrene from the samples was checked by extensive washing with cyclohexane until no pyrene was found in the supernatant. The concentration of the pyrene in the supernatant was monitored by absorption spectrometry using the absorption peak of pyrene at 336 nm. The extent of leaching was followed over a period of weeks (Table 1).

Gas Adsorption Measurements. Measurements were carried out on a Micromeritics ASAP 2000 surface area analyzer both with N_2 and with CO_2 . Samples were degassed for extended periods of time (2–3 days) at 40 °C. The equilibration time for the samples was adjusted until the desorption branch reunited with the adsorption branch. The equilibration time cited here is the time that the apparatus waits until within a predetermined tolerance, no change in pressure (constant in all these measurements), takes place.

Oxygen Penetration Measurements. The rate of oxygen penetration was followed by measuring the pyrene fluorescence of precooled (–130 to –185 °C) doped xerogels exposed to an excess of oxygen. The oxygen quenches the pyrene fluorescence, causing a reduction in the initial intensity of the fluorescence decay and, to a lesser extent, a reduction in the lifetime, τ . Samples of the doped xerogel were placed in a long-stemmed fluorescence cuvette which was placed within an Oxford Instrument DN-1000 cryostat. The sample was attached to a vacuum system by means of a flexible hose and kept under a vacuum of ~ 1 mTorr at 60 °C for several days. Degassing of the sample was continued until reproducible results were observed. After degassing, the sample was dosed with 700 Torr of helium and the temperature reduced. Helium was placed in the sample cuvette to ensure efficient thermal equilibration. Pressure measurements were made by means of a Baratron MKS pressure transducer with a 1000-Torr full-scale range. Temperature was controlled with a resistive heater within the cryostat, controlled by a Eurotherm temperature controller with a resolution of 0.1 °C.

The fluorescence decay of the pyrene was measured from the front face of the sample after excitation with the 337-nm line of a nitrogen laser (PRA LN-1000). Fluorescence was collected through a 370-nm interference filter and a monochromator onto a Hamamatsu multichannel plate and digitized by a Tektronix 7912 oscilloscope. The data were collected and processed on a PC. The fwhm of the system was ~ 1 ns.

After helium evacuation the fluorescence without quencher was measured and the vacuum system filled with oxygen at 500 Torr up to the stopcock leading to the sample. The experiment was initiated by opening the stopcock and allowing the oxygen to expand into the sample. The fluorescence decays were then collected over a period of time ranging from a few minutes to several hours depending on the sample and temperature. In samples with the higher penetration rates, measurements were made with a program that automatically saved the fluorescence decay along with the time at each laser pulse. Sample C (Table 1), the sample with the lowest penetration rates, was manually ground and sieved, and particles of 3–4-mm diameter were used. Samples A and B, with penetration rates that were at the upper range of our measurement resolution, were measured as irregular shards of the xerogel monolith.

Results

Gas Adsorption Measurements. The N_2 adsorption isotherm measured for sample A, (Figure 1a), using standard equilibration times (5 s), was of type II, indicative of a mesoporous solid,⁸ with a clear hysteresis loop. At these standard equilibration times, sample B showed a rising desorption branch (Figure 1b), indicating that the sample had not reached equilibrium. On extension of equilibration to 200 s, a type I (Langmuirian) isotherm was observed (Figure 1c), typical of highly microporous materials. The measurement of a single point may take a few hours at an equilibration time of 200 s (see Experimental Details), and the measurement of a full isotherm 48 h. Similarly for sample C, N_2 adsorption did

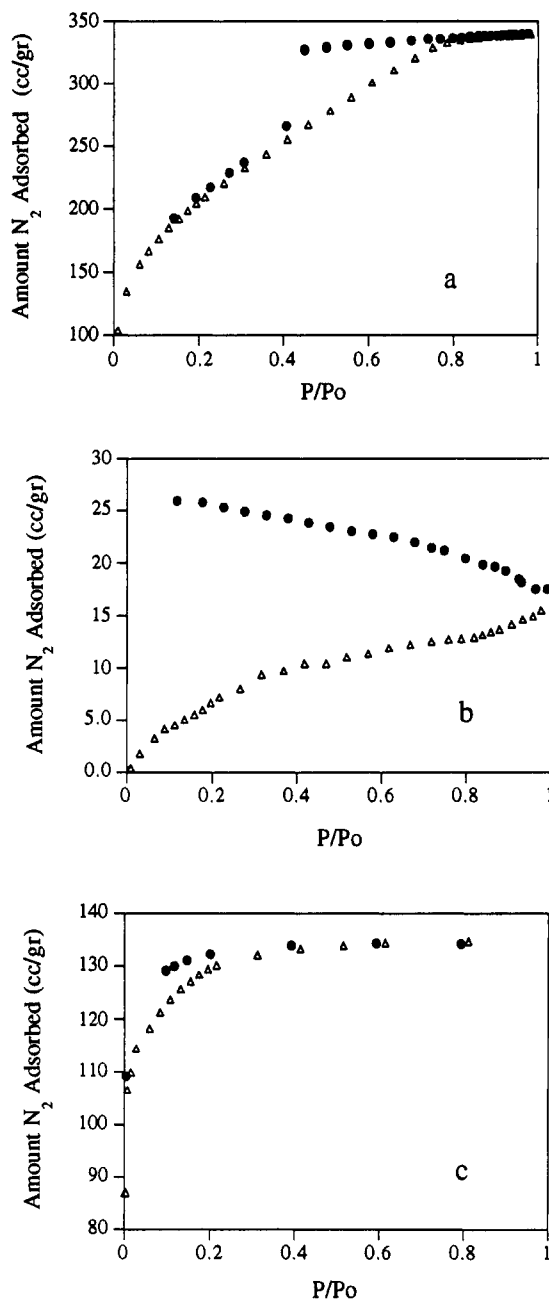


Figure 1. Adsorption–desorption N_2 isotherms for two pyrene-doped SiO_2 xerogels. (Δ) Adsorption; (\bullet) desorption. (a) Xerogel A, 5-s equilibration time. (b) Xerogel B, 5-s equilibration time. (c) Xerogel B, 150-s equilibration time.

not reach equilibrium within reasonable equilibration times and a rising desorption branch was observed. The problem of N_2 equilibration in gas adsorption measurements on microporous solids is well documented in the area of coal and carbon research⁹ and is attributed to high activation energy of diffusion of the N_2 molecule, which causes very long equilibration times at the temperature of liquid nitrogen at which these measurements are usually carried out. This phenomenon has recently been observed in Si based xerogels as well.¹⁰ To overcome this problem, termed “activated diffusion”, CO_2 isotherms were measured.¹¹ Owing to the lower P_0 of CO_2 at higher temperatures it is possible to measure CO_2 isotherms at 0 °C up to a P/P_0 of 0.03. As may be seen in Figure 2, the desorption branch follows the adsorption branch, indicat-

(10) Sharp, K. G. *J. Sol-Gel Sci. Tech.*, in press.

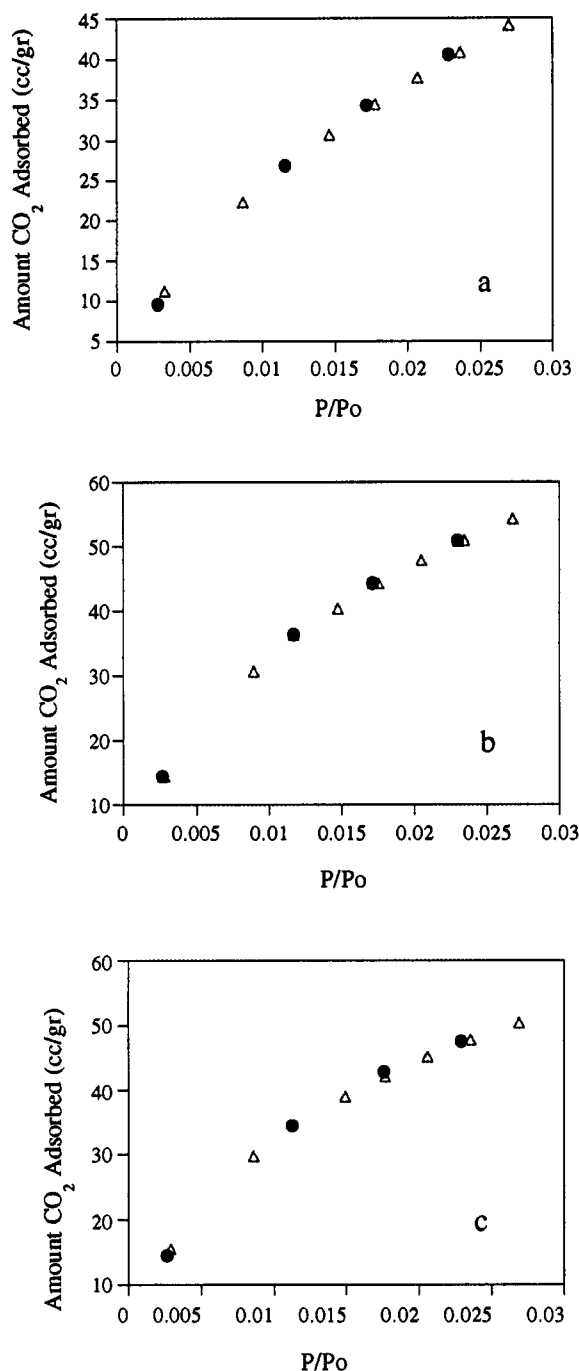


Figure 2. Adsorption-desorption CO_2 isotherms measured at 0°C . (Δ) Adsorption; (\bullet) desorption. (a) Xerogel A.; (b) xerogel B; (c) xerogel C.

ing that equilibration has been reached. The results of all surface area measurements and pore size analyses are collected in Table 1.

Fluorescence Measurements. It is important to distinguish between two time domains in this experiment. The first time domain is that of the fluorescence lifetime of the excited pyrene, up to ~ 200 ns. The second time domain is that of the O_2 penetration into the xerogel and is on the order of seconds to hours depending on the type of xerogel and on the temperature. The fluorescence decays of the unquenched pyrene are well described by a single exponent with a lifetime, τ , of 205 ± 5 ns (Figure

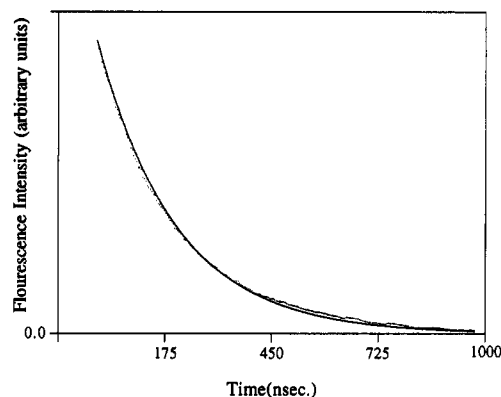


Figure 3. Decay profile (\cdots) of unquenched pyrene fluorescence in xerogel C at -160°C . The fit ($-$) to a single exponent.

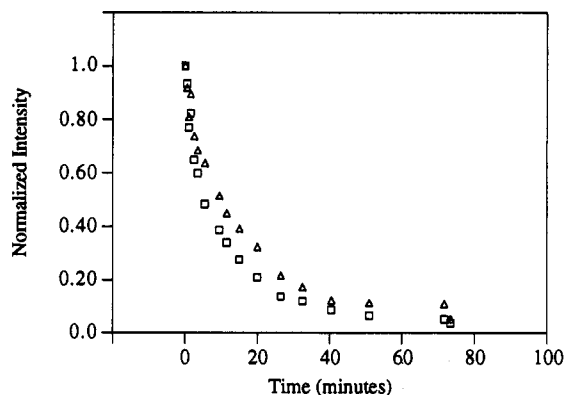


Figure 4. Drop in the relative integrated intensity, $F(\text{py})$, of the fluorescence decay of pyrene, and initial relative intensity, Δ , both for sample C, precooled to -150°C after exposure to oxygen.

3). Upon introduction of oxygen there is a drop in initial intensity, a reduction in the observed lifetime and the fluorescence decay becomes highly nonexponential. The ratio of the area beneath the quenched decay and the unquenched decay gives the remaining fraction of pyrene, $F(\text{py})$, that has not reacted with oxygen:

$$F(\text{py}) = \int_0^\infty I_q dt / \int_0^\infty I_0 dt$$

where $I_0(t)$ is the intensity of the unquenched decay and $I_q(t)$ is the intensity of the quenched decay. Exposure of the pyrene-doped sample to O_2 causes a drop in $F(\text{py})$. As the oxygen penetrates into the xerogel, more of the pyrene, excited with each laser pulse, is quenched. Thus, with repeated pulsed laser excitation of the pyrene, the ratio $F(\text{py})$ drops, following the slow entrance of the oxygen into the doped xerogel (Figure 4). In addition one may plot the drop in the ratio of the initial intensities (Figure 4). As can be seen, the two plots are quite similar, indicating that the transient component, which is responsible for the drop in the initial intensity and which is beyond the resolution of our system (~ 1 ns), is far greater than the drop in lifetime which is within our temporal resolution. $F(\text{py})$ entails both the initial drop in intensity and the time-resolved component, and as the extent of the dynamic component alters with temperature and from sample to sample, the intensity decay plots, for all samples, are given as the drop in $F(\text{py})$.

For samples A and B (Figure 5), it is seen that at -185°C the drop in $F(\text{py})$ is on the order of seconds and minutes, respectively. A pronounced temperature effect was measured for sample C (Figure 6). At the lowest temperature

(11) Fahrenholtz, W. G.; Smith, D. M.; Duen-Wu, Hua *J. Non-Cryst. Solids* 1992, 144, 45.

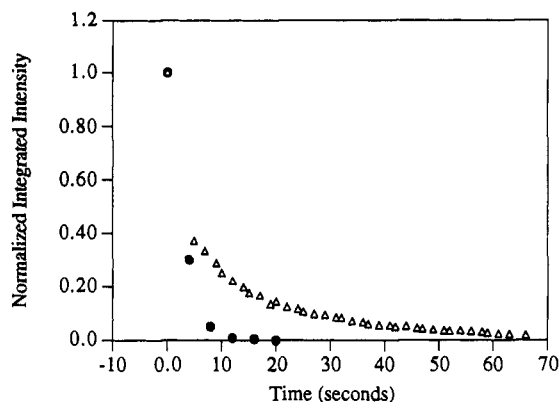


Figure 5. Integrated intensity of pyrene fluorescence, $F(\text{py})$, in two xerogels pre-cooled to $-185\text{ }^\circ\text{C}$ after exposure to oxygen, (●) xerogel A; (Δ) xerogel B.

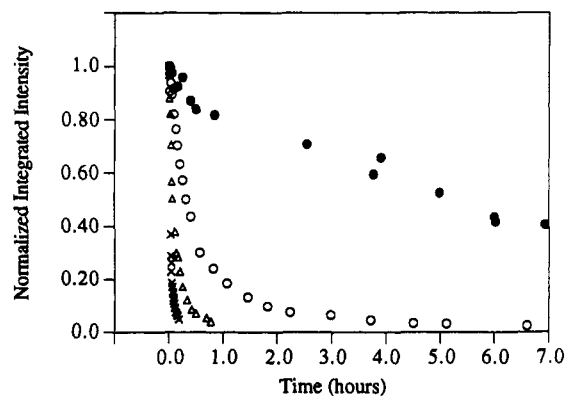


Figure 6. Drop in the integrated pyrene fluorescence intensity, $F(\text{py})$, in sample C upon exposure of a pre-cooled sample to an excess of oxygen. (×) $-130\text{ }^\circ\text{C}$; (Δ) $-150\text{ }^\circ\text{C}$; (○) $-160\text{ }^\circ\text{C}$; (●) $-170\text{ }^\circ\text{C}$.

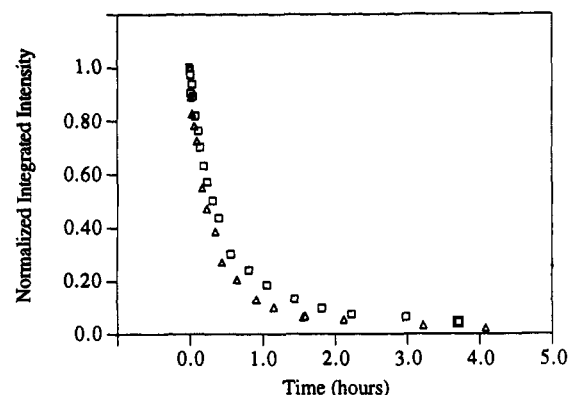


Figure 7. $F(\text{py})$ for xerogel C at $-160\text{ }^\circ\text{C}$ as a function of time. Comparison of two experiments.

measured, $-170\text{ }^\circ\text{C}$, the decay took place over a period of hours while at $-130\text{ }^\circ\text{C}$ the decay in $F(\text{py})$ was still an order of magnitude greater than that observed in sample B at $-185\text{ }^\circ\text{C}$. In these experiments it is important to ascertain that the measured decrease in $F(\text{py})$ is not a function of degassing and that the results are reproducible after continued evacuation of the sample. An example of reproducibility after additional evacuation may be observed in Figure 7. One of the main observations is that the quenching of the pyrene, after a long enough time, is essentially complete in all three xerogels.

The marked temperature dependence measured for xerogel C allows one to perform an Arrhenius analysis of activation energy. The full kinetic description of $F(\text{py})$

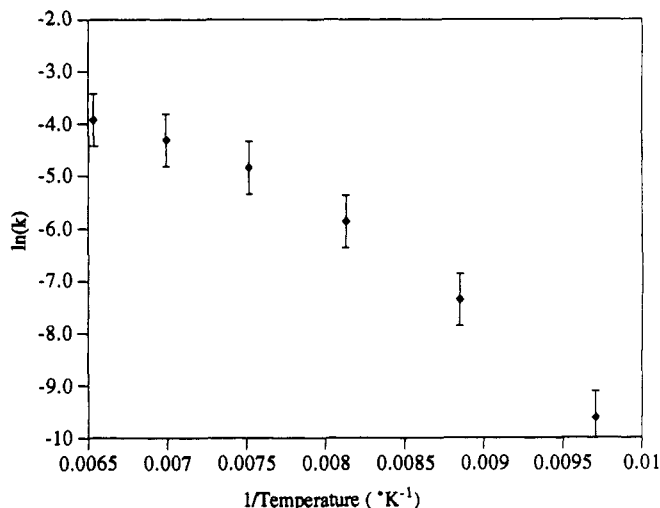


Figure 8. Arrhenius-type graph of the rate of the drop in integrated pyrene fluorescence in xerogel C as a function of temperature.

is complex, and should take into account both the diffusion of the oxygen into the sample and the oxygen concentration dependence of $F(\text{py})$. However, the decays were found empirically to fit reasonably well to a first-order description, and this was employed for the Arrhenius plot as is shown in (Figure 8). It is seen that the upper part of the plot is bent (see Discussion). The activation energy for the O_2 penetration was taken from the lower part of the plot, and was found to be $18 \pm 1\text{ kJ/mol}$.

Discussion

The nitrogen adsorption results on the three xerogels do not enable us to compare the average pore size distribution (apd) by any method of calculation because it is not possible to measure the N_2 isotherm liquid nitrogen temperatures on xerogel C within a reasonable period of time. Going from xerogel A to B, a drop in the apd is observed, and the isotherm shape changes from that typical of a partially mesoporous solid, to that typical of a solid that is highly microporous. The extreme microporosity of sample C may be inferred from the fact that there is an appreciable surface area measured with CO_2 (similar to the CO_2 surface area in sample B) that is not measurable with N_2 . Increased microporosity in samples prepared with higher acidity of the starting solution in TMOS or TEOS xerogels, has been observed previously.¹² Here we add that a reduction in the water/TMOS ratio causes a decrease in pore dimensions as well. The rate of the increase in the extent of oxygen quenching after exposure of the samples to oxygen, or the rate the drop of $F(\text{py})$, correlates with the adsorption measurements: Sample A has a rate of drop in $F(\text{py})$ greater by a factor of more than 3 orders of magnitude, compared to that of sample B at a temperature of $-170\text{ }^\circ\text{C}$.

The fluorescence quenching experiments were carried out with a large excess of oxygen. For quenching to take place, oxygen must reach the vicinity of an excited pyrene molecule. While the drop in fluorescence is related to the rate of diffusion, it is not possible to estimate the actual value of these rates. This is for two reasons: first, the distances that an oxygen molecule traverses are not known;

second, the extent of quenching in a heterogeneous system is often not a linear function of concentration of the quencher.

While it is not possible to give absolute diffusion rates, the activation energy of diffusion may be assessed for a given sample, because here we are observing the *change* of the rate of penetration with temperature. The Arrhenius type plot of the rate in the drop of $F(\text{py})$ is not linear as measured for sample A. The curved plot, particularly at higher temperatures, may indicate a change in the mechanism of transport of the oxygen. However, at lower temperatures, the linear part of the plot (four lower points) gives an activation energy of 18 ± 1 kJ/mol. This is greater than the barrier for oxygen diffusion on mesoporous silica¹³ (8 kJ/mol), determined by means of analysis of the surface diffusion controlled reaction between excited $\text{Ru}(\text{bpy})_3^{2+}$ and oxygen. The greater value for the barrier for diffusion in the xerogel is a reflection of the high microporosity of the material. It is important to note, however, that the above diffusion coefficients measured for oxygen on mesoporous silica are for short-range diffusion (limited by the lifetime of the excited state of the $\text{Ru}(\text{bpy})_3^{2+}$, ~ 500 ns), while the diffusion barrier measured for oxygen on the xerogel is for long-range diffusion, measured over a period of hours. In heterogeneous systems long-range and short-range diffusion rates may be different. It will be interesting, in future work, to apply diffusion controlled reactions, to assess the short-range diffusion coefficients on the xerogel and to compare them to the present long-range diffusion values.

While, as stated above, it is impossible to estimate rates of diffusion, the large qualitative difference in the rate of penetration of the oxygen into the samples, particularly the difference between samples A and B and sample C

may be interpreted as the effect of xerogel surface geometry on the rate of diffusion of oxygen into the sample. The xerogel prepared with the most highly acidic catalyst and lowest water/TMOS ratio has the slowest rate of diffusion of oxygen.

Regardless of starting conditions, the oxygen quenching of the pyrene in the resultant xerogel is total. If the pyrene was truly situated within the bulk of the xerogel, it would be expected that a certain part of the pyrene would be inaccessible to oxygen. The total accessibility of the pyrene, indicates that during the formation of the xerogel the pyrene, possibly because of its nonpolar nature, migrates and is trapped at the pore surface.

Conclusion

The pyrene doped by a sol-gel process within a silica xerogel remains totally accessible to oxygen quenching, regardless of xerogel starting conditions. The xerogel starting conditions effect the geometric characteristics of the resultant xerogel and the leachability of the pyrene. At low pH low water/TMOS ratios pyrene does not leach out of the xerogel at all. This finding, which is remarkable for a hydrophobic molecule such as pyrene, leads to a nonleachable reactive doped xerogel. The method, by which the quenching of excited state pyrene is monitored after exposure of a precooled sample to an excess of oxygen, enabled us to determine the activation energy for the diffusion of oxygen into a xerogel as 18 ± 1 kJ/mol.

Acknowledgment. Supported by the US-Israel Bi-national Foundation and by the Ministry of Science and Technology. J.S. thanks the Valtazi Pikovski foundation for their generous support. D.A. and M.O. are members of the Farkas Center for Light Energy Conversion. D.A. is also a member of the F. Haber Research Center for Molecular Dynamics.

(13) Samuel, J.; Avnir, D.; Ottolenghi, M. *J. Phys. Chem.* **1992**, *96*, 6398.